Supplemental Figure 1

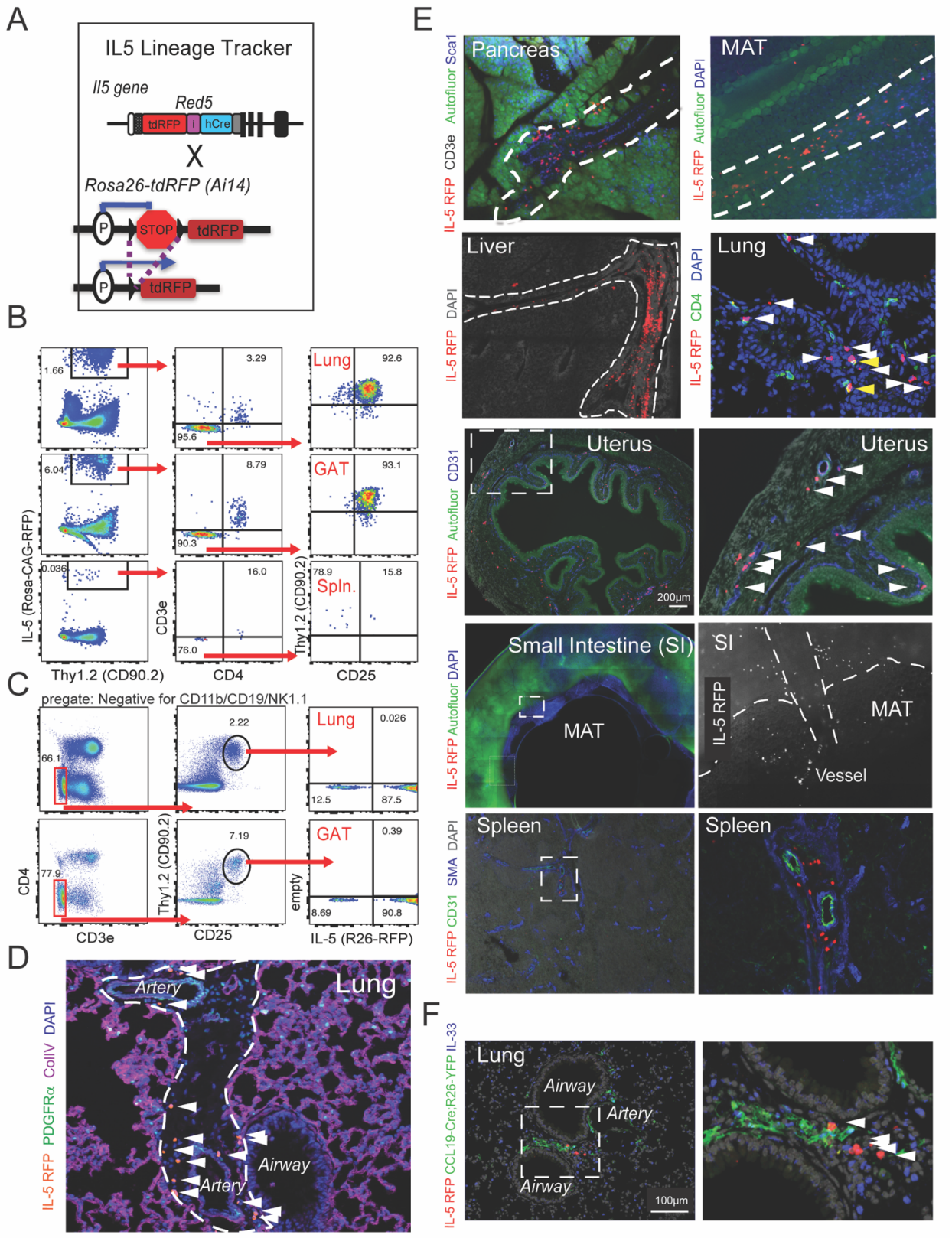

Figure S1, Related to Fig. 1: Distribution of ILC2s in cuffs of multiple non-barrier organs. (**A**). Schematic of IL-5Cre-tdtomato; R26-CAG-tdtomato (Ai14) lineage-tracker-mouse reporter line. (**B and C**) Flow cytometry analysis of mouse from (**A**) demonstrating >90% specificity (**B**) and ~90% sensitivity (**C**) of the reporter in lung, perigonadal adipose tissue (GAT), and spleen (Spln). (**D**) 2D thin-cut lung imaging of ILC2s (IL-5RFP$^+$) in Collagen IV-negative arterial adventitial cuff. (**E**) 2D thin-cut imaging of ILC2s (IL-5 RFP$^+$) and rare Th2 cells (IL-5 RFP$^+$ CD4$^+$, yellow arrowheads) in cuffs from pancreas, mesenteric adipose tissue (MAT), liver, uterus, small intestine (SI), and spleen. (**F**) 2D thin-cut imaging of (ILC2) IL-5 RFP$^+$ cells and CCL19-Cre; R26-YFP$^+$ SC in lung cuffs. (**B-F**) Images and flow cytometry plots are representative of three or more mice.

Supplemental Figure 2

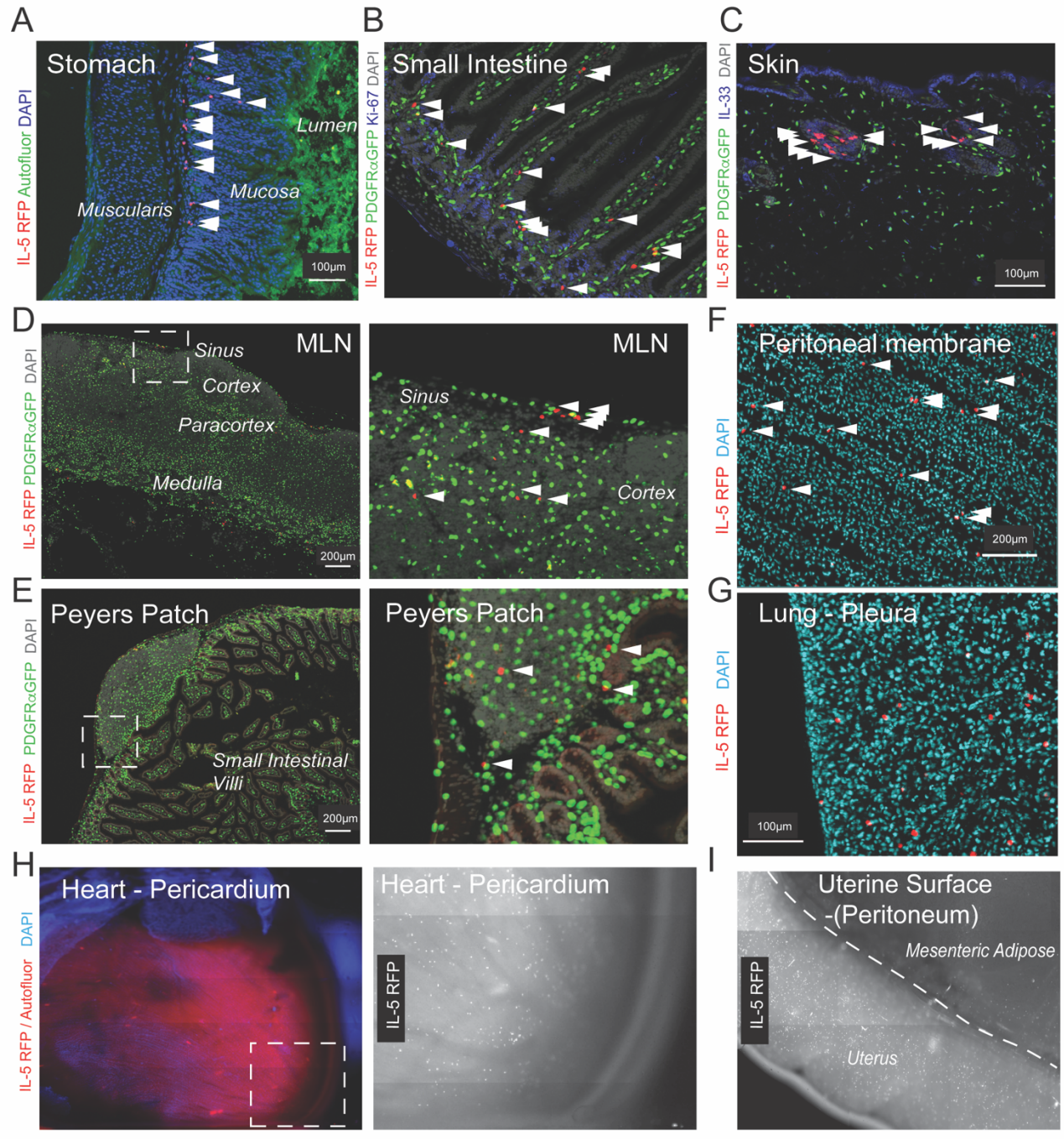

Figure S2, Related to Fig. 1: Distribution of ILC2s in epithelial, serosal body-cavity sites, and secondary lymphoid organs (SLOs). (**A-C**) 2D thin-cut imaging of ILC2 (IL-5RFP$^+$) in 'epithelial tissues', including (**A**) stomach at the boundary of the muscularis and mucosa layers, (**B**) small intestine (SI) villus and epithelial crypts (marked with Ki-67), and (**C**) skin hair follicles. (**D-E**) 2D thin cut-imaging of ILC2 (IL-5RFP$^+$) in SLOs, including (**D**) mesenteric lymph node (MLN) and (**E**) peyers patches of the SI. (**F-I**) 2D thin-cut imaging of ILC2 in serosal body cavity membranes, including (**F**) peritoneal membrane, (**G)** visceral pleura of the lung, (**H**) pericardium of the heart, or (**I**) peritoneal surface of the uterus. In some cases, PDGFRαGFP$^+$ stromal cells were also visualized as noted. Images are representative of two or more mice.

Supplemental Figure 3

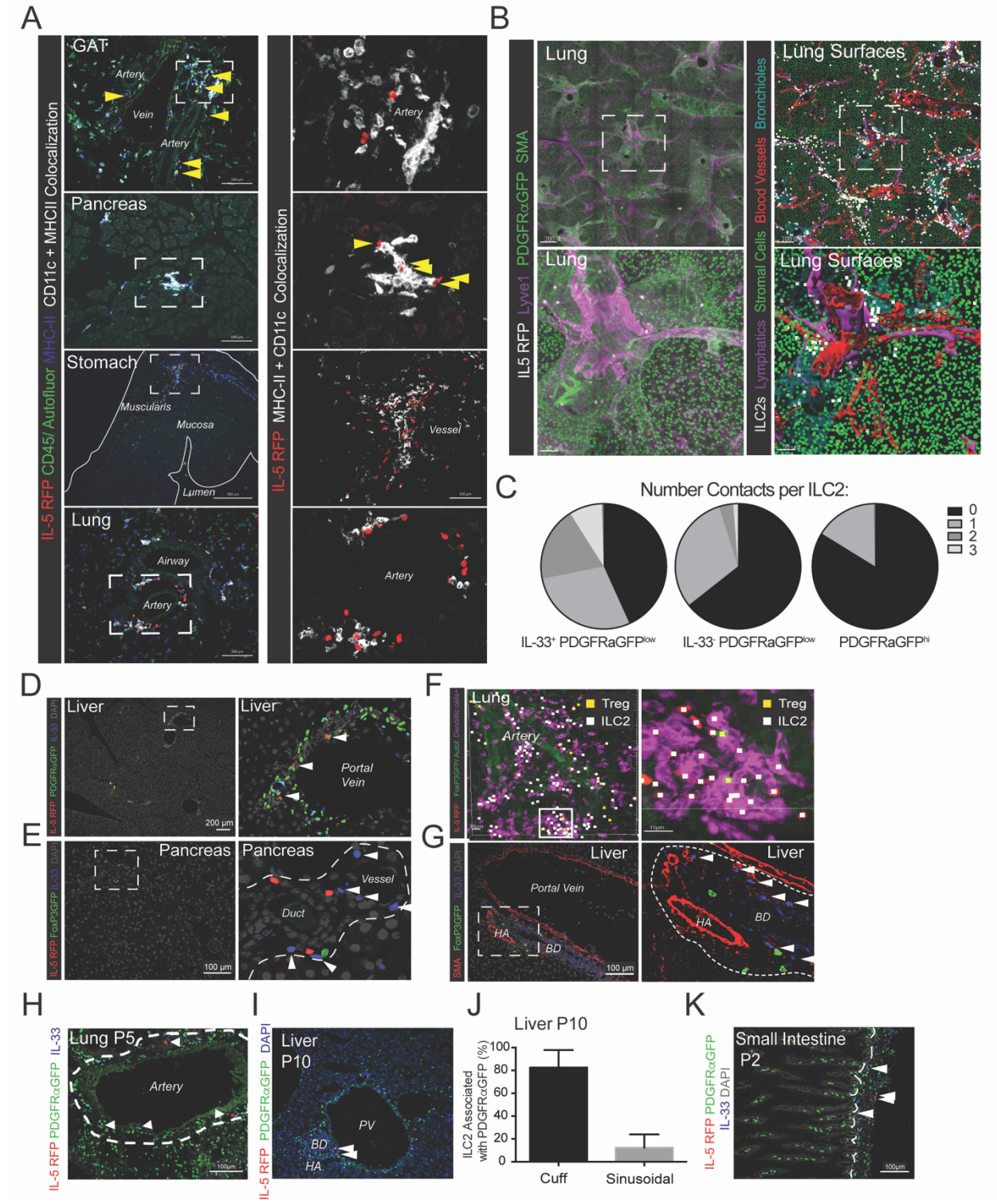

Figure S3, Related to Figs 1-3: (**A**) 2D thin-cut imaging of ILC2 (IL-5RFP+ CD45+) and dendritic cells (DCs; $CD45^+$ $CD11c^+$ $MHCII^+$) in gonadal adipose tissue (GAT), pancreas, stomach and lung. (**B**) 3D imaging from lung of a 200μm projection of (top) a large lung survey with PDGFRαGFP, SMA, IL-5 RFP, and Lyve1 showing airways, arteries, veins, and lymphatics. Images were analyzed by utilizing co-localization channels and surfacing in Imaris software. Surfaces were rendered on SMA^+ airways, SMA^+, $Lyve1^+$ blood vessels, SMA^-, $Lyve1^+$ lymphatic vessels, GFP^+ PDGFRα stromal cells, and IL-5 RFP^+ ILC2s. (Bottom) A close up of an airway-artery bundle with surfaces in place. (**C**) Analysis of 3D images related to Fig 3A-D, demonstrating number of contacts per ILC2 (IL-5 RFP^+) with the indicated stromal subset. (**D-G**) Localization of ILC2s, DC and Treg subsets, and IL-33+ ASCs in indicated tissues. (**F**) 3D rendering with zoom of a 200μm thick projection with IL-5 RFP+ ILC2, Tregs (FoxP3GFP+), and DCs ($CD11c^+$ $MHCII^+$). (**D,G**) 2D thin cut images of liver and (**E**) pancreas identified ILC2 (IL-5 RFP^+) and Tregs ($CD3\varepsilon^+$ $FoxP3GFP^+$) in proximity to $IL\text{-}33^+$ ASCs. (**H-K**) 2D-thin cut images from tissues showing localization of PDGFRαGFP cells and IL-5RFP+ ILC2s during postnatal developmental time points indicated; (**H**) P5 lung, (**I**) P10 liver, or (**K**) P2 small intestine. (**J**) Quantification of localization of cuff (left) and sinusoidal (blood-borne, right) ILC2s (IL5 RFP^+) with PDGFRαGFP$^+$ SCs in P10 liver. Images are representative of three or more mice.

Supplemental Figure 4

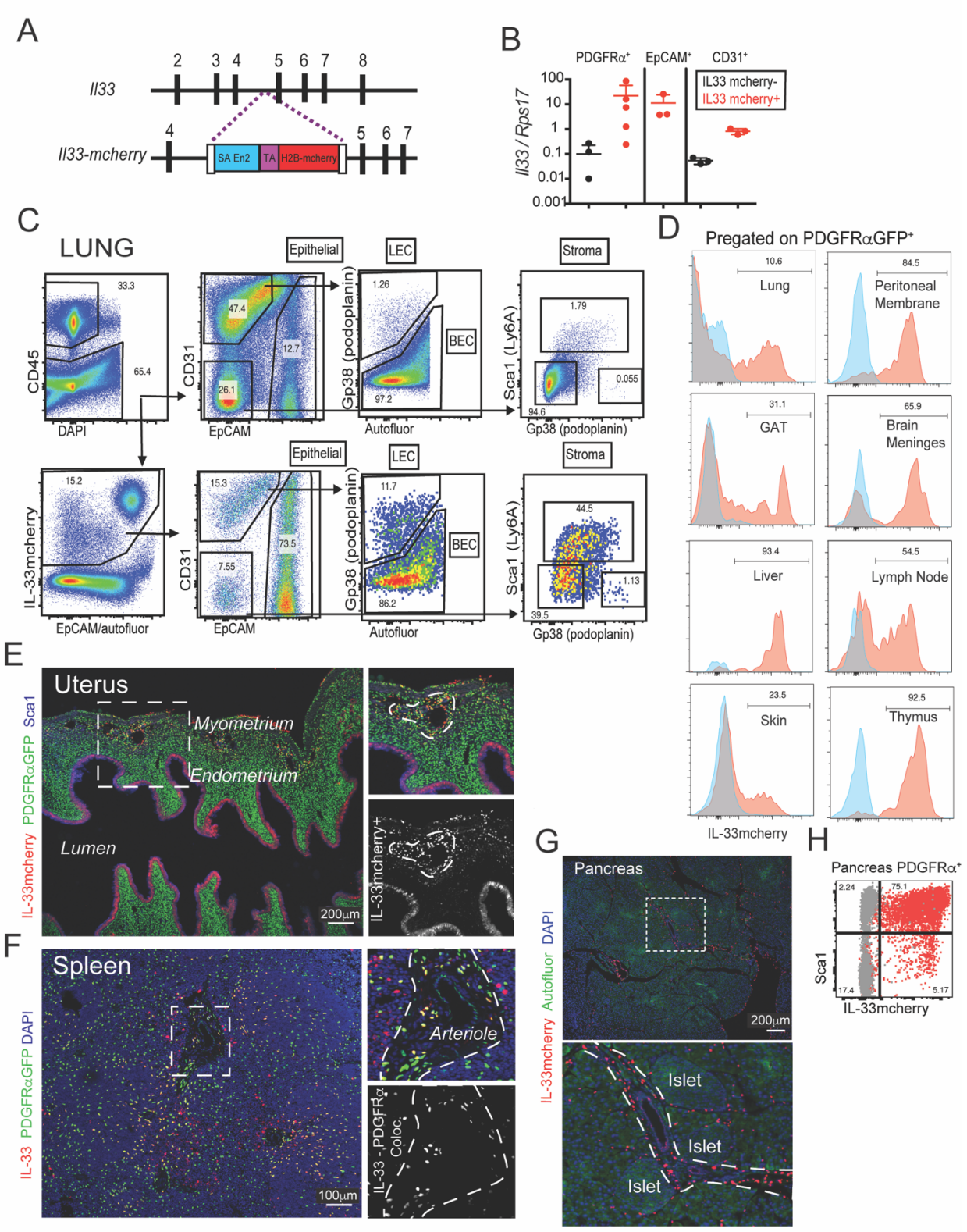

Figure S4, Related to Fig 4: IL-33mcherry reporter construction, validation, and analysis via imaging and flow cytometry (**A**) Diagram of the construction for the IL-33-H2B-mcherry nuclear localization IL-33 reporter (**B**) qPCR validation of *Il33* transcript from sorted cells of the indicated IL-33mcherry^{+} (red) and cherry- (black) populations. (**C**) Flow cytometry analysis of lungs from IL-33mcherry heterozygous mice, demonstrating (top) subsets of epithelia, endothelia (blood BEC and lymphatic LEC), and stromal subsets, with (bottom) breakdown of all IL-33mcherry^{+} cells within these categories. (**D**) Flow cytometry from indicated tissues pre-gated on all PDGFRαGFP^{+} stromal cells and demonstrating IL-33mcherry subset expression (or reporter negative wild-type gating control). (**E-G**) Thin-cut imaging of IL-33 expression in adventitial cuffs of (**E**) uterus (non-pregnant), (**F**) spleen, and (**G**) pancreas revealed PDGFRα^{+} IL-33^{+} cells present in the cuff. **(H)** Flow cytometry analysis of pancreas from IL-33mcherry homozygous (red) or wild-type control (grey) mice identified a dominant mesenchymal subset of Sca1^{+} IL-33^{+} ASCs. Images and flow cytometry plots are representative of 3 experiments. **(B)** pooled data from 3 independent experiments.

Supplemental Figure 5

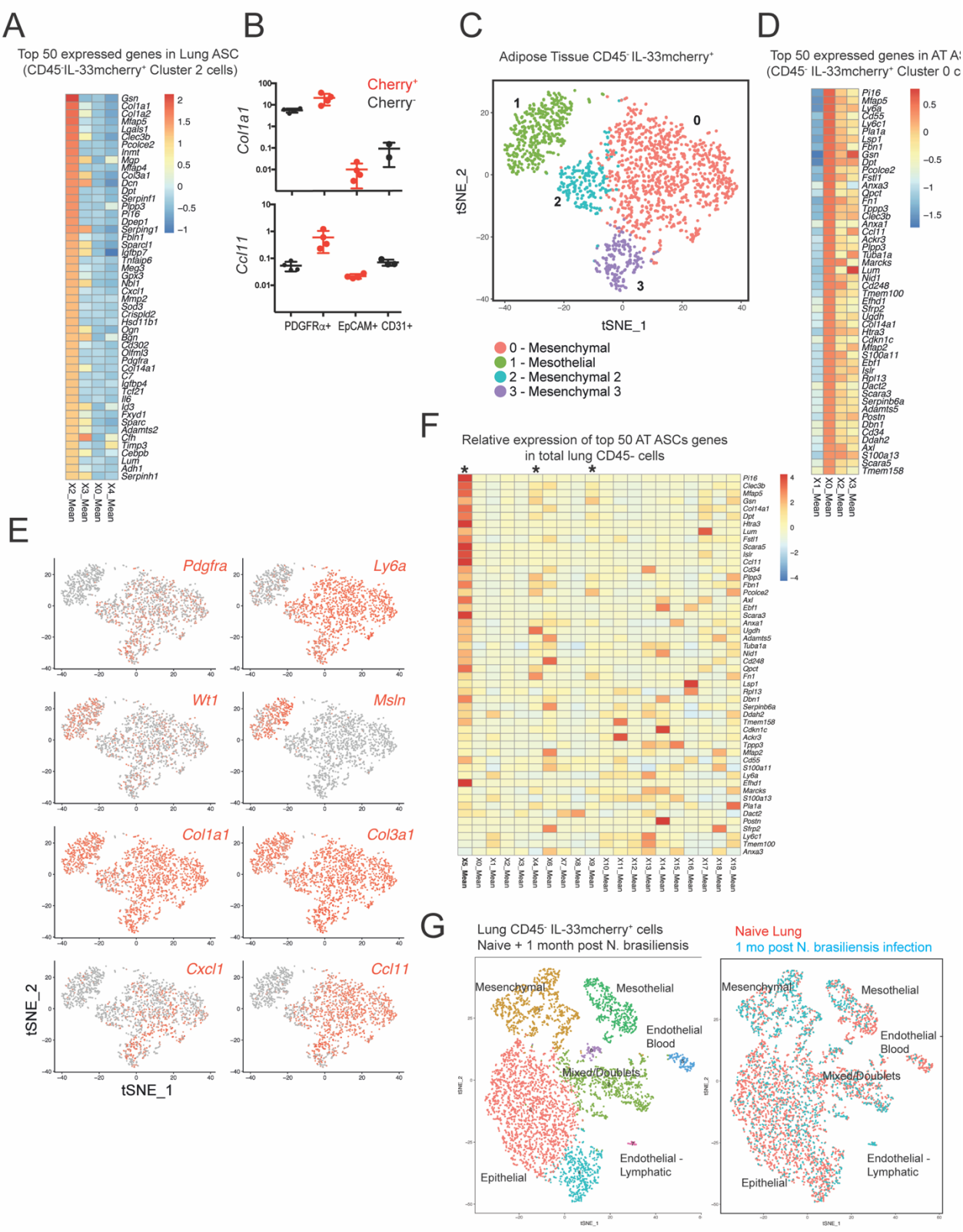

Figure S5, Related to Fig 5: scRNA seq of adipose tissue ASCs resemble lung ASCs. **(A**) Heatmap of mean expression values of top 50 genes in lung ASCs (cluster 5). Data is log- transformed. (**B**) Validation of *Col1a1* and *Ccl11* mRNA expression by qPCR on sorted IL-33^{+} and IL-33^{-} subsets of lung mesenchymal (PDGFRα^{+}), epithelial (EpCAM^{+}) and endothelial (CD31^{+}) cells. (**C**) Unsupervised clustering analysis of IL-33mcherry+ CD45- cells from perigonadal adipose tissue (GAT) visualized with t-SNE. Each dot indicates an individual cell (total cell number: 2037). (**D**) Heatmap of mean expression values of top 50 genes in GAT ASCs. Data is log- transformed. (**E**) Gene expression of selected genes projected onto tSNE plots. (**F**) Heatmap of mean expression values of top 50 genes in GAT ASCs projected on total lung CD45^{-} cell clusters. Data is log-transformed and row normalized. Stars indicate the three lung mesenchymal clusters (4, 5, and 9) and correspond to those described in Fig 5E. (**G**) Unsupervised clustering analysis of aggregated lung samples (IL-33mcherry^{+} CD45^{-} cells) from naïve and 4 weeks post *N. Brasiliensis* infection visualized with t-SNE. Each dot indicates an individual cell (total cell number: 5287). Cells are colored based on clusters (left panel) or sample origin (right panel).

Supplemental Figure 6

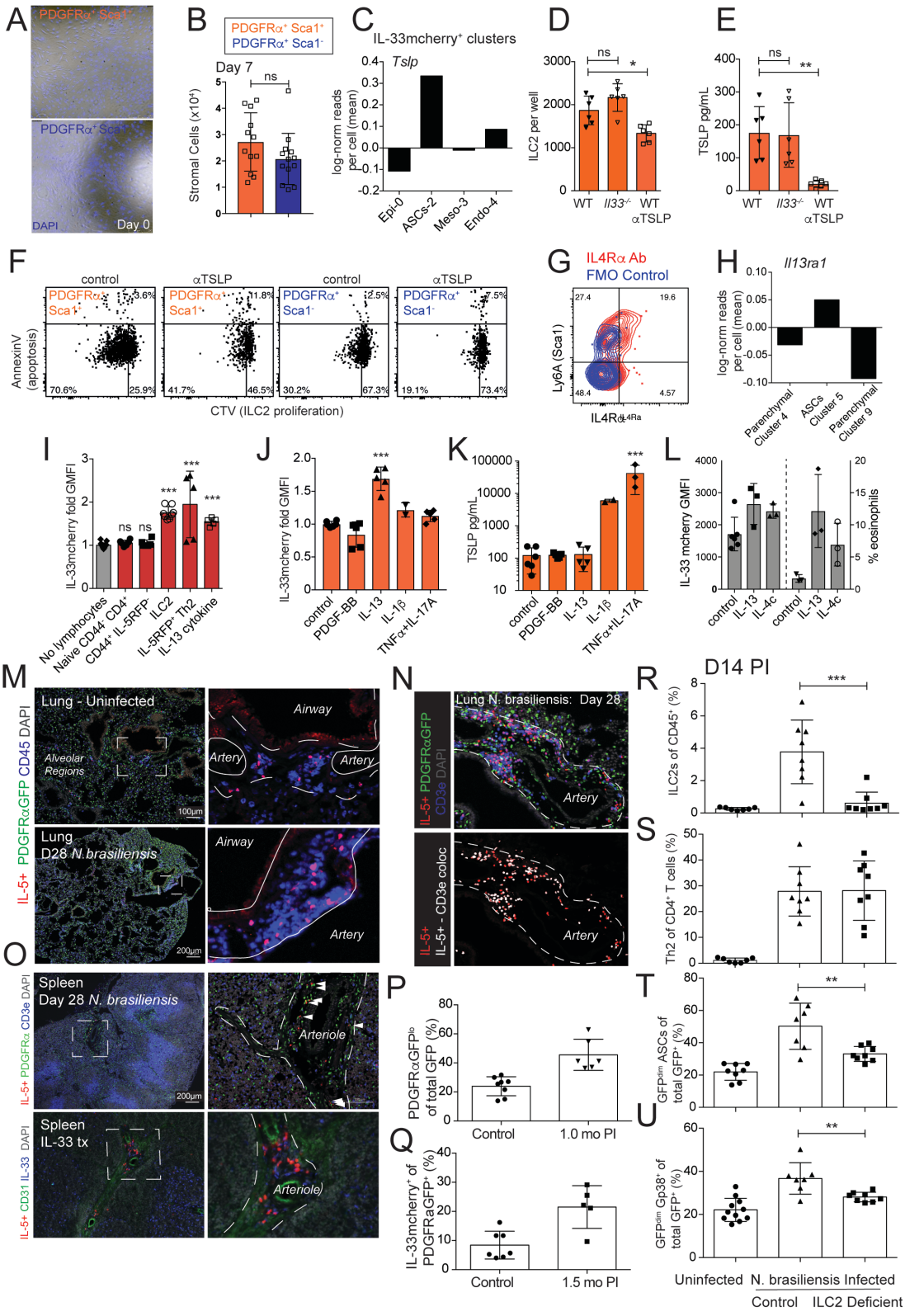

Figure S6, Related to Fig 6: (A and B) Monolayers of ASCs (PDGFRα$^+$Sca1$^+$, orange) and parenchymal enriched stromal cells (PDGFRα$^+$Sca$^-$, blue) at **(A)** ILC2 seeding and **(B)** enumerated 7 days post-seeding. (**C**) Log-normalized *Tslp* reads per cell from lung IL-33mcherry$^+$ scRNAseq clusters defined in Fig 5A. (**D**) ILC2s and (**E**) TSLP amounts in ASC-ILC2 7-day co-cultures from wild-type (WT), IL-33 deficient, or wild-type treated with anti-TSLP blocking antibody. (**F**) Day 5 ILC2 proliferation (CTV dilution) and apoptosis (annexin V) analysis from ILC2 supernatant cultures +/- anti-TSLP. **(G and H**) ASC expression of IL-13 receptor components, with (**G**) IL4Rα, shown by flow cytometry, or (**H**) *Il13ra,* shown as log-normalized reads from scRNAseq in Fig 5E. (**I-J**) ASCs IL-33mcherry expression (GMFI) and (**K**) culture supernatant TSLP amounts after co-culture with the indicated lymphocytes or treatment with the indicated cytokines at 10ng/mL for (**I**) 5 or (**J and K**) 3 days. (**L**) IL-33mCherry expression and frequency of eosinophils (percent of CD45$^+$ cells) in lungs from IL-33mcherry heterozygous mice treated with IL-13 or IL-4complex i.n. for seven days, analyzed 20hrs post final dose. (**M and N**) Thin cut lung images from naive mice and day 28 post *N. brasiliensis* infection and stained for the indicated markers, demonstrating accumulation of cuff ILC2s (IL5RFP$^+$ CD3e$^-$), IL-5$^+$ Th2 cells (IL5RFP+ CD3e$^+$), and total CD45$^+$ hematopoietic cells. (**O**) ILC2s (IL-5RFP$^+$ CD3e$^-$) in spleen day 28 post *N. brasiliensis* or day 6 post IL-33 treatment (500ng x3). (**P-U**) Flow cytometry analysis of lungs from the indicated time points post *N. brasiliensis* infection, demonstrating (**P**) relative percent of PDGFRαGFP^{lo} cuff ASCs, (**Q**) total stromal cell IL-33mCherry expression, or (**R-U**) post-infection frequencies of (**R**) ILC2s, (**S**) Th2 cells, (**T**) GFP-dim ASCs, or (**U**) GFP-dim GP38+ ASC subset from control (*Il5-cre*) or ILC2 deficient (*Il5-cre*;R26-DTA) mice. All images and flow cytometry plots are representative of three or more mice, bar graphs are pooled data from 2-3 experiments.

Supplemental Figure 7

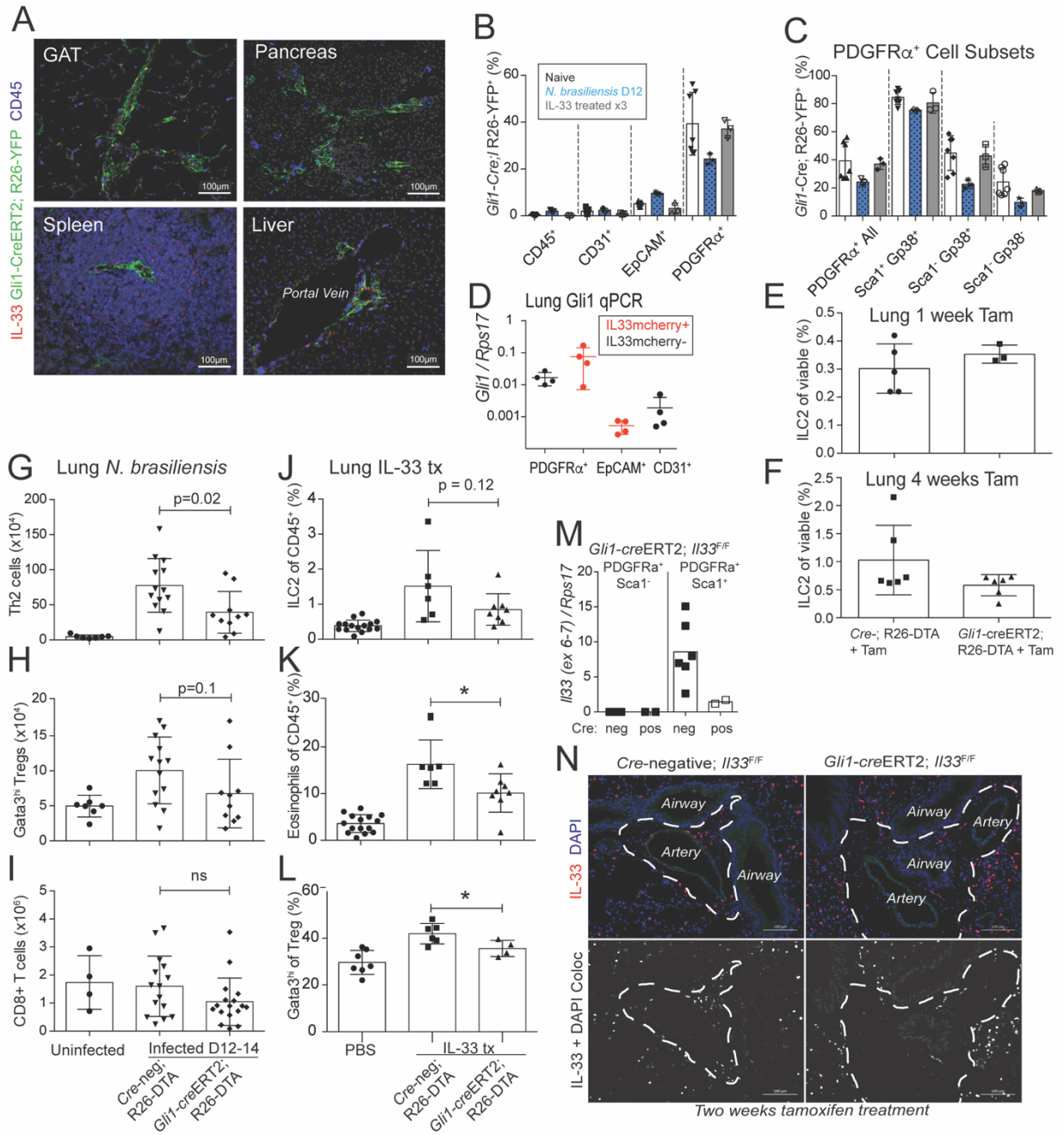

Figure S7, Related to Fig 7: (**A**) 2D thin-cut images of tamoxifen treated (x3 doses) *Gli1-cre*ERT2; R26-YFP from perigonadal adipose tissue (GAT), pancreas, spleen, and liver. (**B and C**) Percentage Gli1^{-}YFP^{+} cells of indicated populations analyzed by flow cytometry from naive mice (black), IL-33 treated (x3 500ng doses over 6 days, grey), or day 12 post *N. brasiliensis* infection (blue). (**D**) qPCR analysis of *Gli1* from the indicated sorted SC subsets from lung (black, IL-33mcherry-negative; red, IL-33mcherry^{+}). (**E and**

F) Flow cytometry analysis of ILC2 numbers (**E**) one week or (**F**) four weeks post tamoxifen induction of Gli1^{+} cell deletion. (**G-L**) Flow cytometry analysis of tamoxifen treated Gli1-deleter mice and littermate controls after (**J-L**) IL-33 treatment (500ng x3 and PBS controls or (**G-I**) *N. brasiliensis* infection PI D12-14. (**M**) qPCR on sorted stromal cells from lungs of *Gli1-cre*ERT2; IL-33 Flox mice. (**N**) 2D thin-cut imaging of lungs from *Gli1-cre*ERT2; IL-33 Flox and Cre-negative littermate controls, stained for IL-33. (**A,N**) Representative of three or more mice. (**B and C**) One representative of three experiments shown, (**D-M**) pooled data from three or more independent experiments, with individual mice shown. * $p<0.05$, ** $p<0.01$, or indicated.

Table S1, Related to Fig 5: Complete scRNAseq results for all clusters defined. Tabs for 1) lung IL-33mcherry^{+} 2) lung total CD45^{-} 3) GAT IL-33mcherry^{+} 4) Lung naïve and day 30 PI *N. brasiliensis* 5) DAVID GO analysis for total lung cluster 5 ASCs.

Movie S1, Related to Fig 1: Meningeal ILC2s: 3D

Movie S2, Related to Fig 1: Pancreas ILC2s: serial Z stack sections

Movie S3, Related to Fig 3: Lung ILC2s with cuff stromal cells: serial Z stack sections

Movie S4, Related to Fig 3: GAT ILC2s with IL-33 expressing stroma: 3D